



ELSEVIER

Nuclear Instruments and Methods in Physics Research A 480 (2002) 65–70

**NUCLEAR
INSTRUMENTS
& METHODS
IN PHYSICS
RESEARCH**
Section A

www.elsevier.com/locate/nima

VUV reflective coatings on thin concave float glass substrates with a perimeter of 86 cm to be used as provisional HADES RICH mirror segments

P. Maier-Komor*, J. Friese, R. Gernhäuser, J. Homolka, A. Kastenmüller, H.J. Körner, A. Ulrich, K. Zeitelhack

Physik-Department E12, Technische Universität München, James Franck Strasse, D-85747 Garching, Germany

Abstract

The setup in the UHV box coater for the HADES RICH mirrors was modified to deposit VUV reflective layers on large area substrates. These substrates were made of 2 mm thick float glass with 87 cm spherical curvature and a perimeter of 86 cm. A good uniformity of the coatings could be obtained by a larger source-to-substrate distance of 155 cm. Impurity problems due to lower deposition rates had to be avoided with a better process vacuum. The modified setup, the thickness calibrations, uniformity tests, process conditions and reflectivity measurements are presented. © 2001 Elsevier Science B.V. All rights reserved.

PACS: 81.15; 29.40.K; 68.55.L; 07.30.K

Keywords: Aluminum; Electron beam evaporation; Optical measurements; Resistance heated source; RICH detector; Titanium; Thickness by quartz crystal monitor; VUV reflectivity

1. Introduction

The high-acceptance di-electron spectrometer (HADES) [1], presently installed at the GSI Darmstadt, has reached a status where commissioning and the first experiments should be possible. The RICH detector in which relativistic leptons are selectively identified was developed and built at our institute.

The main challenges were to develop:

- (a) CsI photon converter films with high quantum efficiency in a gaseous environment,
- (b) a CaF₂ window, 5 mm thick, of 1.4 m diameter with $\approx 75\%$ transmittance for VUV light at 145 nm wavelength,
- (c) a highly polished spherical mirror with low z substrate material, 2 mm thickness, 1.5 m diameter and the pertinent reflective coating with VUV reflectance $> 80\%$.

If one of these main challenges could not have been met, the RICH detector would not have functioned and thus the whole HADES project would have failed. The successful development of

*Corresponding author. Tel.: +49-89-2891-2436; fax: +49-89-2891-2297.

E-mail address: peter.maier-komor@physik.tu-muenchen.de (P. Maier-Komor).

high efficiency CsI photon converters was described in Refs. [2–5], and that of the VUV mirrors in Refs. [6,7].

Since the 18 glassy carbon (SIGRADUR®) segments (50% of which have not been funded as yet) for the HADES RICH mirror could not be produced or polished in time, a back-up solution was necessary. Industrial firms which manufacture shaving mirrors and rear-view mirrors for cars were able to produce spherical mirrors of float glass with acceptable optical quality at reasonable costs. Thus, segments of 2 mm thick float glass with 87 cm spherical curvature and a perimeter of 86 cm could be produced. Each of these large segments covers one sixth of the solid angle of the HADES RICH mirror and compensates thus for three SIGRADUR® panels. Such large mirror substrates still fitted in the UHV box coater [6,7] and could even be rotated therein for better thickness homogeneity.

2. Improvement of the vacuum system of the UHV box coater

An acceptable uniformity of the coatings on the glass substrates with a perimeter of 86 cm could be obtained by enlarging the source-to-substrate distance from 87 cm to 155 cm. Thus, the condensation rate was reduced to $\approx 30\%$ of the previous value for the same evaporation rate. Lower deposition rates cause higher impurity contents in the Al as well as in the MgF_2 films, owing to the impingement of residual gases. This had to be avoided by providing a better process vacuum.

The weak point in the evacuating process was the bake-out procedure, during which an insufficient pumping speed was at first provided by a hybrid turbomolecular pump backed by a diaphragm pump. Independently of whether the bake-out procedure lasted 5 or 8 h, the cross-over vacuum to the cryopump was never better than 5×10^{-3} Pa. This indicates that the dominant partial pressure comes from water vapor, as proved in Ref. [3] by comparing the vacuum values with the filled liquid nitrogen cold wall and without the liquid nitrogen. In the previous case,

the vacuum improved from 3×10^{-7} Pa to 5×10^{-8} Pa with the liquid nitrogen filling.

There was no flange on the UHV box coater to install a bigger turbomolecular pump. Therefore, a second hybrid turbomolecular pump (DN 100 CF, 200 l/s pumping speed) with a second diaphragm pump was installed. When the modified setup was leak tested another weak point of the pump system came to the fore. The leak detector was installed in the fore-line of the turbomolecular pump (D1) (see Fig. 1). Whenever the gate valve (12) of (D2) was closed the background level decreased in the leak detector indicating an interruption of backstreaming from the poor vacuum maintained by the diaphragm pump (E2). That is why the fore-lines

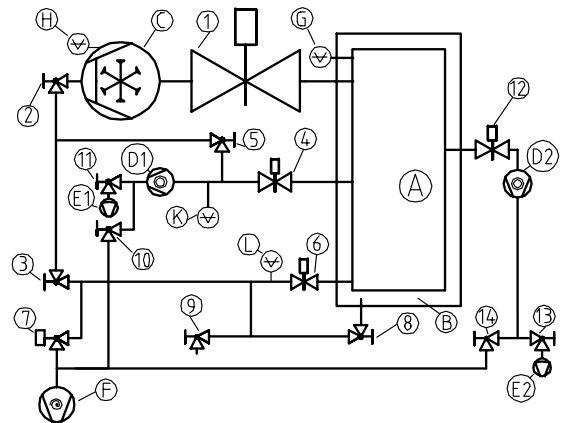


Fig. 1. Diagram of the upgraded pump system for the UHV box coater: (A) deposition chamber, (B) differential pumping volume for the viton sealed front gate, (1) bellows sealed gate valve with 50 cm \varnothing free opening, (C) UHV cryopump, (2) regeneration valve of the cryopump, (3) right angle valve for isolation of the regeneration line from the roughing line, (4) bellows sealed gate valve with 10 cm \varnothing free opening, (5) differential high vacuum valve, (D1) and (D2) turbomolecular pumps, (E1) and (E2) diaphragm vacuum pumps, (6) bellows sealed gate valve with 7 cm \varnothing free opening for roughing of the UHV chamber, (7) right angle valve for isolation of the scroll pump from the differential pumping lines for the UHV valves (2) and (6), (8) right angle valve for isolation of the differential volume, (9) vent valve, (F) scroll pump, (G) ionization vacuum gauge I, (H) ionization vacuum gauge II, (K) thermocouple vacuum gauge, (L) convection vacuum gauge, (10) right angle valve for the connection of (F) to the fore-line of (D1), (11) right angle valve for isolation of (E1), (12) bellows sealed gate valve with 10 cm \varnothing free opening, (13) right angle valve for isolation of (E2), (14) right angle valve for the connection of (F) to the fore-line of (D2).

of (D1) and (D2) were connected to the scroll pump (F) via the right angle valves (10) and (14), respectively. During evacuation of the box coater with the turbomolecular pumps (D1) and (D2) for the bake-out procedure the scroll pump (F) was their backing pump. Thus, a cross-over vacuum to the cryopump of $\approx 1 \times 10^{-3}$ Pa instead of the former 5×10^3 Pa could be reached after 7 h bake-out time. After the bake-out procedure the turbomolecular pumps (D1) and (D2) were used only to provide differential pumping to all viton gaskets, which were exposed to ultra-high vacuum. These are the inner gasket of the front gate and the valve seats of (2), (4), (6) and (12). For the differential pumping purpose, the diaphragm pumps (E1) and (E2) are sufficient as backing pumps. They were utilized, because they have longer service intervals than the scroll pump. Thus, the scroll pump (F) was required only for the main roughing and the bake-out procedure. Due to the better bake-out procedure a final vacuum of $\approx 9 \times 10^{-8}$ Pa could be reached, and with the filled liquid nitrogen cold wall, even $\approx 4 \times 10^{-8}$ Pa. The improvement of the vacuum by the cold wall indicates that still more than half of the total pressure is due to water vapor.

During the Al evaporation the highest pressure was then $\approx 1 \times 10^{-5}$ Pa, instead of the former value of $\approx 8 \times 10^{-5}$ Pa without the improved bake-out procedure. Therefore, the impurity content coming from the impingement of residual gases should be now slightly reduced, in spite of the reduced condensation rate (30%).

3. Evaporation setup and procedure

Nothing was changed in the proven setup of the source chamber as reported in Ref. [3]. Also, the power specifications of the sources were reproduced, and thus the evaporation rates. Unfortunately an error in the part number of the MgF_2 source was published in that Ref. [3]. It should actually be the SO-24 evaporation source (Mathis Company, Long Beach, CA). We tried to increase the evaporation rate of Al by increasing the electron beam power from 10 to 11 kW. Due to this power increase, however, the Al melted

completely in its hearth, with the disadvantage that the removal for cleaning could hardly be accomplished. Also, since the evaporation rate increased only by $\approx 10\%$, all the following Al evaporations were done with 10 kW as usual. It was not possible to maintain the position of the thickness sensor head due to mounting problems with the large area substrates. Therefore, this sensor head was dismantled in a reversible way, to be utilized again for the evaporations on the glassy carbon (SIGRADUR[®]) segments. Another UHV quartz sensor head was installed at about the same height as the large float glass panels. This had to be calibrated for the thickness on the rotating substrates, and in the same charge the spatial deposition distribution was determined. For this quartz sensors were mounted on the same concave stainless steel sheet as described in Ref. [3], but now at a source-to-substrate distance of 155 cm instead of 87 cm. For this setup, the thickness inhomogeneity of the Al condensation is $< 6\%$, from the rotation center to a distance of 23 cm from this center, for the MgF_2 -deposition this value is $< 3\%$. Both values show only half as much inhomogeneity as for the case of the lower source-to-substrate distance (87 cm). Since the glass substrates have a perimeter of 86 cm, instead of 50 cm as do the glassy carbon substrates, the total inhomogeneity will not be much better than for the smaller substrates.

With this setup, six concave float glass substrates with a perimeter of 86 cm were coated with the desired VUV reflective coating. The thickness values were $5 \mu\text{g}/\text{cm}^2$ Ti, followed by $20 \mu\text{g}/\text{cm}^2$ Al, protected by $11.5 \mu\text{g}/\text{cm}^2$ MgF_2 . These were the best matched values leading to a reflectivity of $> 80\%$ down to 145 nm wavelength as show in Fig. 10 of Ref. [3]. It was not possible to mount witness samples together with these large glass panels; therefore, no reflectance measurements could be performed for these six deposition charges, and we had to trust the good reproducibility of the deposition process previously demonstrated. Only four glass panels were installed in the HADES RICH detector, the others were not used because of insufficient shape accuracy or insufficient cleaning. It became evident that substrate cleaning is of imminent importance and becomes

more and more complicated with increasing size of the substrate. Even if some contamination is very thin and nearly transparent homogeneously distributed over the glass substrate, it can increase the surface roughness of the deposited film and thus ruin the reflectivity, especially for short wavelengths.

After finishing of the evaporations for the six large glass mirror segments, the quartz sensor head for thickness detection at the lower source-to-substrate distance which was reinstalled in its old position. Then six glassy carbon (SIGRADUR[®]) segments were coated for the subsequent beam time at the GSI. Since we might find improved evaporation conditions for even better VUV reflectivity, we omitted the Ti evaporation, because Ti cannot be removed by HNO₃ or HCl as in the case of the Al and MgF₂ layers. Therefore only 20 μg/cm² Al, protected by 11.5 μg/cm² MgF₂ was deposited. In this setup witness samples could be mounted, and thus the reproducibility of the depositions could be controlled by measuring the reflectance.

As described in Ref. [3] care must be taken that no water film remains on or in the MgF₂ film, when the mirror is placed in vacuum again or in humidity-free gas environment after venting. In some of the films of Ref. [3], it was believed that the MgF₂ layer might have had a permanent water impurity of ≈0.5 μg/cm². This suspicion arose when the reflectance data [3] showed a dip at a wavelength of 165 nm, which excluded an interference pattern but is an indication for water (which has a wide absorption maximum at this wavelength) independent from the thickness of the MgF₂ layer. The permanent water impurity was measured on the quartz of the thickness monitor by comparing its thickness reading after deposition but before venting, with that found after venting and re-evacuating to UHV. This measurement, however, has no relevance for the mirror films, because there the surface roughness is very low in contrast to that of the quartz crystal. Since the evaporated MgF₂ molecules impinged on the quartz crystal at an angle of >30°, some area of the Al layer, which was as well deposited at a much smaller angle as from a large area source, was shaded due to the surface roughness and thus was

not protected by MgF₂. This uncovered Al area was oxidized when venting. This interpretation was obvious when further evaporations with presumably better MgF₂ material also showed the observed effect in the quartz reading. Nevertheless, the reflectivity of the best matched sample (Fig. 10 of Ref. [3]) was reproduced.

4. Reflectivity results and discussion

The setup for the reflectivity measurements as described in Ref. [3] was modified to have the additional capability of being able to measure the reflectivity of concave samples and to have a more representative angle of incidence relative to the application in the HADES RICH detector. Instead of an angle of incidence $\varphi \approx 45^\circ$ a steep incidence of $9^\circ < \varphi < 14^\circ$ was chosen. Fig. 2 shows reflectance data of two samples from different evaporation charges. The filled-circle data points represent the reflectivity of the Al/MgF₂ coatings on a float glass substrate which was a witness sample in a deposition charge for one of the SIGRADUR[®] segments. The vacuum was about the same, and the MgF₂ layer had the same thickness as in the process for the best sample of Ref. [3] (Fig. 10, solid line [3]). Again, a reflectivity of >80% was obtained for wavelengths down to 150 nm. A quartz glass sample (owner: CARL ZEISS, 73446 Oberkochen, Germany) from the same deposition charge completely reproduced the relevant sample of Ref. [3]. The differences in these three samples might be due to slightly different degrees of success in cleaning. The cross-shaped data points for another charge show an unacceptably poorer reflectivity which was also obtained for the other witness samples of the second deposition charge. The latter samples demonstrate the importance of an excellent process vacuum, because during the bake-out procedure a leak occurred which degraded the vacuum by nearly one order of magnitude compared to the other deposition charges.

For the above mentioned quartz glass sample the reflectivity at 157 nm as a function of incident angle was measured by CARL ZEISS [8]. Fig. 3 presents the best fit to their data points

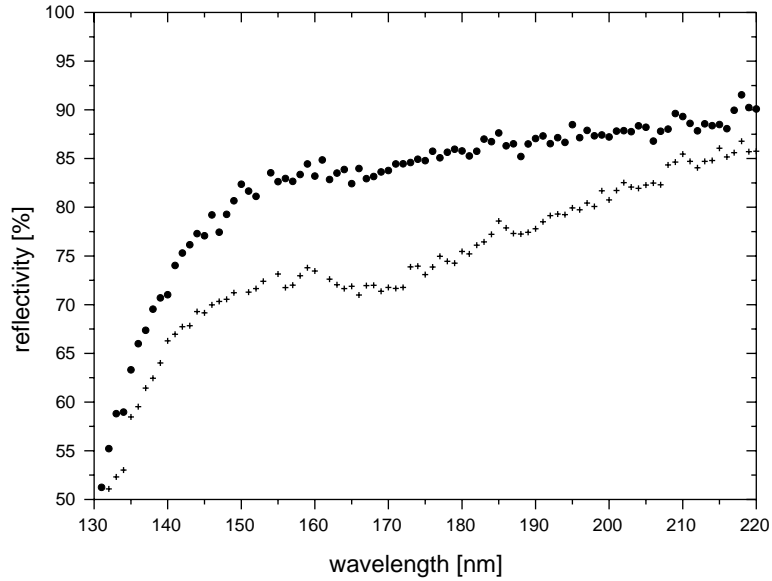


Fig. 2. Reflectivity as a function of wavelength for two samples, both with the optimum MgF_2 thickness. The filled circle data points are for a sample prepared with the best obtainable process vacuum. The cross-shaped data points are for a sample produced in a one order of magnitude poorer vacuum.

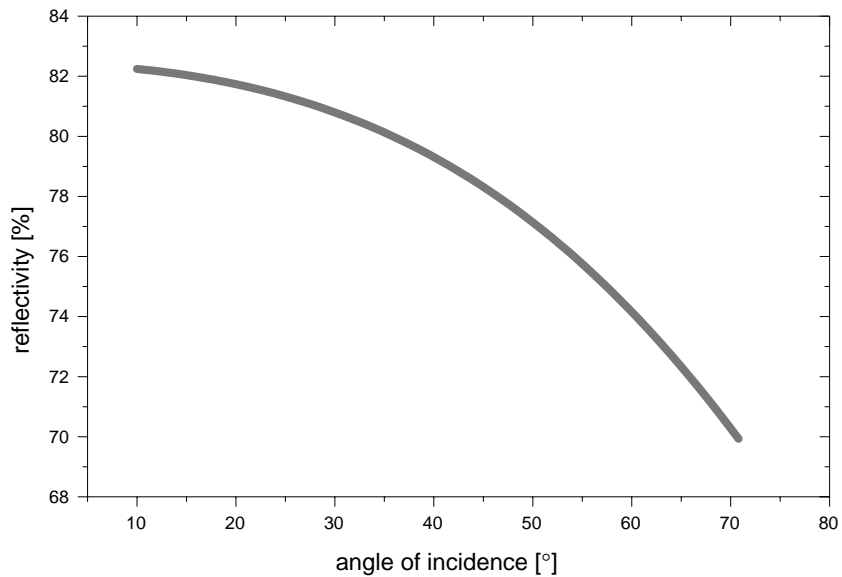


Fig. 3. Reflectivity at 157 nm wavelength as a function of incident angle for a sample of the same deposition charge as shown in Fig. 2 with the better reflectivity.

approximated by the series

$$R = a + b \cos \varphi + c \cos^2 \varphi \quad (1)$$

where R is the reflectivity in %, φ is the angle of incidence, and a , b and c are the fit parameters with the following values for the best fit: $a = 59.8 \pm 0.2$; $b = 34.9 \pm 0.6$ and $c = -12.3 \pm 0.5$.

The reflectivity decreases monotonically with increasing angle of incidence, no interference patterns are observable. This supports our statement in Ref. [3], that the reflectivity as a function of wavelength is not modulated by the influence of interference at the relevant optical thickness of the MgF₂ protection layer. Comparing the reflectivity of this sample at 157 nm with that of the best sample of Ref. [3] should result in $\approx 4\%$ poorer reflectivity for the older sample due to the large angle of incidence during the measurement. This cannot be confirmed, because the different setups do not have the same accuracy in absolute reflectivity measurement.

So far we have no explanation for the slope in Fig. 3; it might come from absorbance in the MgF₂ layer or from surface roughness or from a combination of both effects.

5. Conclusion

The reproducibility of the deposition process concerning the VUV reflectivity is now only slightly better than 10%. There are two reasons which must be investigated. One is the contamination of the surface of the substrates, coming either from insufficient cleaning or from air pollution during longer storage after cleaning. The second reason is related to the cross-over time from the Al to the MgF₂ evaporation. In Ref. [9] a monolayer time for water vapor of approximately 11 s was calculated for a vacuum value similar to that which we had during the VUV mirror coating. Our cross-over time is of the same order, determined mainly by the period required to increase the evaporation rate of the MgF₂ from practically zero

to the working value (by increasing the electric power from $\approx 60\%$ to 100%). Estimating how much one monolayer of water corrodes the Al surface and thus decreases the VUV reflectivity can be investigated by varying the cross-over time. This investigation is planned for the near future and might result in changes of the setup to either shorten the cross-over time or improve of the process vacuum.

Acknowledgements

The authors wish to thank Dr. J. Ullmann and Dr. H. Schink (CARL ZEISS, Oberkochen, Germany) for measuring VUV reflectivities.

This project was supported by the Beschleunigerlaboratorium München and funded by the Freistaat Bayern.

References

- [1] R. Schicker, et al., Nucl. Instr. and Meth. A 380 (1996) 586.
- [2] P. Maier-Komor, B.B. Bauer, J. Friese, R. Gernhäuser, P. Kienle, H.J. Körner, G. Montermann, K. Zeitelhack, Nucl. Instr. and Meth. A 362 (1995) 183.
- [3] J. Friese, R. Gernhäuser, J. Homolka, A. Kastenmüller, P. Maier-Komor, M. Peter, K. Zeitelhack, P. Kienle, H.J. Körner, Nucl. Instr. and Meth. A 438 (1999) 86.
- [4] H. Rabus, U. Kroth, M. Richter, G. Ulm, J. Friese, R. Gernhäuser, A. Kastenmüller, P. Maier-Komor, K. Zeitelhack, Nucl. Instr. and Meth. A 438 (1999) 94.
- [5] R. Gernhäuser, J. Friese, J. Homolka, A. Kastenmüller, P. Kienle, H.J. Körner, P. Maier-Komor, M. Peter, K. Zeitelhack, Nucl. Instr. and Meth. A 438 (1999) 104.
- [6] P. Maier-Komor, A. Bergmaier, G. Dollinger, J. Friese, S. Karsch, P. Kienle, H.J. Körner, Nucl. Instr. and Meth. A 397 (1997) 194.
- [7] P. Maier-Komor, R. Gernhäuser, J. Wieser, A. Ulrich, Nucl. Instr. and Meth. A 438 (1999) 152.
- [8] H. Schink, J. Ullmann, CARL ZEISS, 73446 Oberkochen, Germany, private communication.
- [9] P. Maier-Komor, I. Altarev, A. Bergmaier, G. Dollinger, S. Paul, W. Schott, Nucl. Instr. and Meth. A 480 (2002) 104, these proceedings.